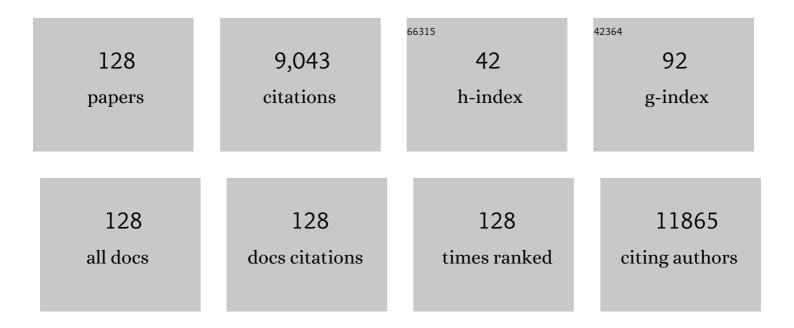
Ze Zhang

List of Publications by Year in descending order

Source: https://exaly.com/author-pdf/3228531/publications.pdf Version: 2024-02-01



ΖΕ ΖΗΛΝΟ

#	Article	IF	CITATIONS
1	Exploring atomic defects in molybdenum disulphide monolayers. Nature Communications, 2015, 6, 6293.	5.8	1,124
2	Tuning element distribution, structure and properties by composition in high-entropy alloys. Nature, 2019, 574, 223-227.	13.7	874
3	Nanoscale origins of the damage tolerance of the high-entropy alloy CrMnFeCoNi. Nature Communications, 2015, 6, 10143.	5.8	608
4	Plasma-assisted fabrication of monolayer phosphorene and its Raman characterization. Nano Research, 2014, 7, 853-859.	5.8	606
5	Formation of monatomic metallic glasses through ultrafast liquid quenching. Nature, 2014, 512, 177-180.	13.7	365
6	Dislocation mechanisms and 3D twin architectures generate exceptional strength-ductility-toughness combination in CrCoNi medium-entropy alloy. Nature Communications, 2017, 8, 14390.	5.8	344
7	Liquid-like pseudoelasticity of sub-10-nm crystalline silver particles. Nature Materials, 2014, 13, 1007-1012.	13.3	255
8	In situ atomic-scale observation of twinning-dominated deformation in nanoscale body-centred cubic tungsten. Nature Materials, 2015, 14, 594-600.	13.3	250
9	Near-ideal theoretical strength in gold nanowires containing angstrom scale twins. Nature Communications, 2013, 4, 1742.	5.8	226
10	Atomic Defects in Twoâ€Dimensional Materials: From Singleâ€Atom Spectroscopy to Functionalities in Optoâ€∤Electronics, Nanomagnetism, and Catalysis. Advanced Materials, 2017, 29, 1606434.	11.1	211
11	Real-time observations of TRIP-induced ultrahigh strain hardening in a dual-phase CrMnFeCoNi high-entropy alloy. Nature Communications, 2020, 11, 826.	5.8	165
12	In situ manipulation of the active Au-TiO ₂ interface with atomic precision during CO oxidation. Science, 2021, 371, 517-521.	6.0	165
13	Reaction and Capacity-Fading Mechanisms of Tin Nanoparticles in Potassium-Ion Batteries. Journal of Physical Chemistry C, 2017, 121, 12652-12657.	1.5	150
14	Visualizing H ₂ O molecules reacting at TiO ₂ active sites with transmission electron microscopy. Science, 2020, 367, 428-430.	6.0	149
15	Capture the growth kinetics of CVD growth of two-dimensional MoS2. Npj 2D Materials and Applications, 2017, 1, .	3.9	115
16	Tracking the sliding of grain boundaries at the atomic scale. Science, 2022, 375, 1261-1265.	6.0	115
17	New twinning route in face-centered cubic nanocrystalline metals. Nature Communications, 2017, 8, 2142.	5.8	110
18	Real-Time Observation of Reconstruction Dynamics on TiO ₂ (001) Surface under Oxygen via an Environmental Transmission Electron Microscope. Nano Letters, 2016, 16, 132-137.	4.5	109

#	Article	IF	CITATIONS
19	Elucidation of Active Sites for CH ₄ Catalytic Oxidation over Pd/CeO ₂ Via Tailoring Metal–Support Interactions. ACS Catalysis, 2021, 11, 5666-5677.	5.5	103
20	Facile synthesis of g-C ₃ N ₄ nanosheets loaded with WO ₃ nanoparticles with enhanced photocatalytic performance under visible light irradiation. RSC Advances, 2017, 7, 24097-24104.	1.7	102
21	In situ atomistic observation of disconnection-mediated grain boundary migration. Nature Communications, 2019, 10, 156.	5.8	98
22	Direct In Situ TEM Visualization and Insight into the Facetâ€Dependent Sintering Behaviors of Gold on TiO ₂ . Angewandte Chemie - International Edition, 2018, 57, 16827-16831.	7.2	92
23	Oxide Catalysts with Ultrastrong Resistance to SO ₂ Deactivation for Removing Nitric Oxide at Low Temperature. Advanced Materials, 2019, 31, e1903719.	11.1	87
24	Slip-activated surface creep with room-temperature super-elongation in metallicÂnanocrystals. Nature Materials, 2017, 16, 439-445.	13.3	82
25	Inâ€Situ Observation of Hydrogenâ€Induced Surface Faceting for Palladium–Copper Nanocrystals at Atmospheric Pressure. Angewandte Chemie - International Edition, 2016, 55, 12427-12430.	7.2	81
26	Piezoresistance behaviors of ultra-strained SiC nanowires. Applied Physics Letters, 2012, 101, .	1.5	79
27	Recent Progresses on Structural Reconstruction of Nanosized Metal Catalysts via Controlled-Atmosphere Transmission Electron Microscopy: A Review. ACS Catalysis, 2020, 10, 14419-14450.	5.5	71
28	An In situ TEM study of the surface oxidation of palladium nanocrystals assisted by electron irradiation. Nanoscale, 2017, 9, 6327-6333.	2.8	68
29	Atomic-resolution imaging of electrically induced oxygen vacancy migration and phase transformation in SrCoO2.5-Ïf. Nature Communications, 2017, 8, 104.	5.8	66
30	Ultrathin Two-Dimensional Pd-Based Nanorings as Catalysts for Hydrogenation with High Activity and Stability. Small, 2015, 11, 4745-4752.	5.2	62
31	Three-dimensional atomic-scale observation of structural evolution of cathode material in a working all-solid-state battery. Nature Communications, 2018, 9, 3341.	5.8	60
32	Facetâ€Dependent Oxidative Strong Metalâ€Support Interactions of Palladium–TiO ₂ Determined by In Situ Transmission Electron Microscopy. Angewandte Chemie - International Edition, 2021, 60, 22339-22344.	7.2	60
33	High-performance hydrogen evolution electrocatalysis by layer-controlled MoS ₂ nanosheets. RSC Advances, 2014, 4, 34733-34738.	1.7	58
34	Metallic nanocrystals with low angle grain boundary for controllable plastic reversibility. Nature Communications, 2020, 11, 3100.	5.8	53
35	Inversion Domain Boundary Induced Stacking and Bandstructure Diversity in Bilayer MoSe ₂ . Nano Letters, 2017, 17, 6653-6660.	4.5	51
36	Recent advances in gas-involved in situ studies via transmission electron microscopy. Nano Research, 2018, 11, 42-67.	5.8	50

#	Article	IF	CITATIONS
37	Anti-twinning in nanoscale tungsten. Science Advances, 2020, 6, eaay2792.	4.7	49
38	In situ atomic-scale observation of grain size and twin thickness effect limit in twin-structural nanocrystalline platinum. Nature Communications, 2020, 11, 1167.	5.8	48
39	Defect-driven selective metal oxidation at atomic scale. Nature Communications, 2021, 12, 558.	5.8	47
40	Direct Atomic-Scale Observation of Ultrasmall Ag Nanowires that Exhibit fcc, bcc, and hcp Structures under Bending. Physical Review Letters, 2022, 128, 015701.	2.9	47
41	Consecutive crystallographic reorientations and superplasticity in body-centered cubic niobium nanowires. Science Advances, 2018, 4, eaas8850.	4.7	46
42	Revealing extreme twin-boundary shear deformability in metallic nanocrystals. Science Advances, 2021, 7, eabe4758.	4.7	46
43	Tuning the Outward to Inward Swelling in Lithiated Silicon Nanotubes via Surface Oxide Coating. Nano Letters, 2016, 16, 5815-5822.	4.5	45
44	Atomic-Scale Observation of Vapor–Solid Nanowire Growth <i>via</i> Oscillatory Mass Transport. ACS Nano, 2016, 10, 763-769.	7.3	43
45	Mesopores induced zero thermal expansion in single-crystal ferroelectrics. Nature Communications, 2018, 9, 1638.	5.8	43
46	Crystal-crystal phase transformation via surface-induced virtual premelting. Physical Review B, 2012, 85, .	1.1	40
47	Mesoporous Fe ₂ O ₃ flakes of high aspect ratio encased within thin carbon skeleton for superior lithium-ion battery anodes. Journal of Materials Chemistry A, 2015, 3, 14178-14187.	5.2	40
48	In Situ STEM Determination of the Atomic Structure and Reconstruction Mechanism of the TiO ₂ (001) (1 × 4) Surface. Chemistry of Materials, 2017, 29, 3189-3194.	3.2	40
49	Vertical/Planar Growth and Surface Orientation of Bi ₂ Te ₃ and Bi ₂ Se ₃ Topological Insulator Nanoplates. Nano Letters, 2015, 15, 3147-3152.	4.5	39
50	The Exceptional Strong Face-centered Cubic Phase and Semi-coherent Phase Boundary in a Eutectic Dual-phase High Entropy Alloy AlCoCrFeNi. Scientific Reports, 2018, 8, 14910.	1.6	39
51	Atomic-scale observation of non-classical nucleation-mediated phase transformation in a titanium alloy. Nature Materials, 2022, 21, 290-296.	13.3	38
52	Surface study of the reconstructed anatase TiO2 (001) surface. Progress in Natural Science: Materials International, 2021, 31, 1-13.	1.8	36
53	Direct Imaging of Kinetic Pathways of Atomic Diffusion in Monolayer Molybdenum Disulfide. Nano Letters, 2017, 17, 3383-3390.	4.5	34
54	Hierarchical twinning governed by defective twin boundary in metallic materials. Science Advances, 2022. 8	4.7	33

#	Article	IF	CITATIONS
55	Layer-dependent anisotropic electronic structure of freestanding quasi-two-dimensional <mml:math xmlns:mml="http://www.w3.org/1998/Math/MathML"><mml:mrow><mml:mi>Mo</mml:mi><mml:msub><mml:m mathvariant="normal">S<mml:mn>2</mml:mn></mml:m </mml:msub></mml:mrow>. Physical Review B, 2016, 93, .</mml:math 	ⁱⁱ 1.1	32
56	In-situ fabrication of Mo6S6-nanowire-terminated edges in monolayer molybdenum disulfide. Nano Research, 2018, 11, 5849-5857.	5.8	32
57	Fast Gas–Solid Reaction Kinetics of Nanoparticles Unveiled by Millisecond Inâ€Situ Electron Diffraction at Ambient Pressure. Angewandte Chemie - International Edition, 2018, 57, 11344-11348.	7.2	31
58	Nanoscale Behavior and Manipulation of the Phase Transition in Singleâ€Crystal Cu ₂ Se. Advanced Materials, 2019, 31, e1804919.	11.1	31
59	In situ interface engineering for probing the limit of quantum dot photovoltaic devices. Nature Nanotechnology, 2019, 14, 950-956.	15.6	30
60	Temperature Effect on Stacking Fault Energy and Deformation Mechanisms in Titanium and Titanium-aluminium Alloy. Scientific Reports, 2020, 10, 3086.	1.6	29
61	In situ atomic scale mechanical microscopy discovering the atomistic mechanisms of plasticity in nano-single crystals and grain rotation in polycrystalline metals. Ultramicroscopy, 2015, 151, 94-100.	0.8	28
62	Probing the oxidative etching induced dissolution of palladium nanocrystals in solution by liquid cell transmission electron microscopy. Micron, 2017, 97, 22-28.	1.1	28
63	Size-dependent dislocation–twin interactions. Nanoscale, 2019, 11, 12672-12679.	2.8	28
64	Timely and atomic-resolved high-temperature mechanical investigation of ductile fracture and atomistic mechanisms of tungsten. Nature Communications, 2021, 12, 2218.	5.8	27
65	In Situ Observation on Dislocation-Controlled Sublimation of Mg Nanoparticles. Nano Letters, 2016, 16, 1156-1160.	4.5	26
66	Deriving phosphorus atomic chains from few-layer black phosphorus. Nano Research, 2017, 10, 2519-2526.	5.8	26
67	Unexpected refacetting of palladium nanoparticles under atmospheric N ₂ conditions. Chemical Communications, 2018, 54, 8587-8590.	2.2	24
68	Electrostatic Force–Driven Oxide Heteroepitaxy for Interface Control. Advanced Materials, 2018, 30, e1707017.	11.1	23
69	Twinning-assisted dynamic adjustment of grain boundary mobility. Nature Communications, 2021, 12, 6695.	5.8	23
70	Direct observation of Pt nanocrystal coalescence induced by electron-excitation-enhanced van der Waals interactions. Nano Research, 2014, 7, 308-314.	5.8	22
71	Discrete shear band plasticity through dislocation activities in body-centered cubic tungsten nanowires. Scientific Reports, 2018, 8, 4574.	1.6	22
72	Dislocation "Bubble-Like-Effect―and the Ambient Temperature Super-plastic Elongation of Body-centred Cubic Single Crystalline Molybdenum. Scientific Reports, 2016, 6, 22937.	1.6	21

#	Article	IF	CITATIONS
73	Superplasticity in Gold Nanowires through the Operation of Multiple Slip Systems. Advanced Functional Materials, 2018, 28, 1805258.	7.8	21
74	Processing, Microstructures and Mechanical Properties of a Ni-Based Single Crystal Superalloy. Crystals, 2020, 10, 572.	1.0	21
75	Grain boundaries in chemical-vapor-deposited atomically thin hexagonal boron nitride. Physical Review Materials, 2019, 3, .	0.9	21
76	Inâ€Situ Observation of Hydrogenâ€Induced Surface Faceting for Palladium–Copper Nanocrystals at Atmospheric Pressure. Angewandte Chemie, 2016, 128, 12615-12618.	1.6	20
77	Surface Energy Driven Liquid-Drop-Like Pseudoelastic Behaviors and In Situ Atomistic Mechanisms of Small-Sized Face-Centered-Cubic Metals. Nano Letters, 2019, 19, 292-298.	4.5	20
78	Cubic-like BaZrO3 nanocrystals with exposed {001}/{011} facets and tuned electronic band structure for enhanced photocatalytic hydrogen production. Journal of Materials Science, 2019, 54, 1967-1976.	1.7	19
79	Discrete twinning dynamics and size-dependent dislocation-to twin transition in body-centred cubic tungsten. Journal of Materials Science and Technology, 2022, 106, 33-40.	5.6	19
80	Direct observation of structural transitions in the phase change material Ge ₂ Sb ₂ Te ₅ . Journal of Materials Chemistry C, 2016, 4, 9303-9309.	2.7	18
81	Atomistic dynamics of sulfur-deficient high-symmetry grain boundaries in molybdenum disulfide. Nanoscale, 2017, 9, 10312-10320.	2.8	18
82	Unveiling the gas-dependent sintering behavior of Au-TiO2 catalysts via environmental transmission electron microscopy. Journal of Catalysis, 2020, 388, 84-90.	3.1	18
83	Observation of enhanced carrier transport properties of Si ⟠100⟩-oriented whiskers under uniaxial strains. Applied Physics Letters, 2014, 104, .	1.5	17
84	Oxidation of <scp><scp>ZrB</scp></scp> ₂ Nanoparticles at High Temperature under Low Oxygen Pressure. Journal of the American Ceramic Society, 2014, 97, 2360-2363.	1.9	17
85	Direct In Situ TEM Visualization and Insight into the Facetâ€Dependent Sintering Behaviors of Gold on TiO ₂ . Angewandte Chemie, 2018, 130, 17069-17073.	1.6	17
86	In situ observation of temperature-dependent atomistic and mesoscale oxidation mechanisms of aluminum nanoparticles. Nano Research, 2020, 13, 183-187.	5.8	17
87	In situ TEM observation of dissolution and regrowth dynamics of MoO2 nanowires under oxygen. Nano Research, 2017, 10, 397-404.	5.8	16
88	A termination-insensitive and robust electron gas at the heterointerface of two complex oxides. Nature Communications, 2019, 10, 4026.	5.8	16
89	Organic–Organic Hybrid g-C ₃ N ₄ /Ethanediamine Nanosheets for Photocatalytic H ₂ Evolution. Journal of Physical Chemistry C, 2018, 122, 24725-24731.	1.5	15
90	Free-Standing Two-Dimensional Gold Membranes Produced by Extreme Mechanical Thinning. ACS Nano, 2020, 14, 17091-17099.	7.3	15

#	Article	IF	CITATIONS
91	Facetâ€Dependent Oxidative Strong Metalâ€Support Interactions of Palladium–TiO 2 Determined by In Situ Transmission Electron Microscopy. Angewandte Chemie, 2021, 133, 22513-22518.	1.6	15
92	Dynamic mechanisms of strengthening and softening of coherent twin boundary via dislocation pile-up and cross-slip. Materials Research Letters, 2022, 10, 539-546.	4.1	15
93	In situ observation of sublimation-enhanced magnesium oxidation at elevated temperature. Nano Research, 2016, 9, 2796-2802.	5.8	14
94	In-situ SEM study of temperature-dependent tensile behavior of Inconel 718 superalloy. Journal of Materials Science, 2021, 56, 16097-16112.	1.7	13
95	<i>In Situ</i> Resolving the Atomic Reconstruction of SnO ₂ (110) Surface. Nano Letters, 2021, 21, 7309-7316.	4.5	13
96	An Environmental Transmission Electron Microscopy Study of the Stability of the TiO ₂ (1) Tj ETQqO	0 0 rgBT /0 1.5	Overlock 10 11
97	Early Stage Growth of Rutile Titania Mesocrystals. Crystal Growth and Design, 2018, 18, 4209-4214.	1.4	10
98	In situ atomic scale mechanisms of strain-induced twin boundary shear to high angle grain boundary in nanocrystalline Pt. Ultramicroscopy, 2018, 195, 69-73.	0.8	9
99	Direct visualization of irreducible ferrielectricity in crystals. Npj Quantum Materials, 2020, 5, .	1.8	9
100	Atomistic dynamics of disconnection-mediated grain boundary plasticity: A case study of gold nanocrystals. Journal of Materials Science and Technology, 2022, 125, 182-191.	5.6	9
101	Hybrid CN-MEA microplates with enhanced photocatalytic hydrogen evolution under visible light irradiation. Catalysis Science and Technology, 2017, 7, 3777-3784.	2.1	8
102	Controllable synthesis of rutile titania with novel curved surfaces. CrystEngComm, 2015, 17, 7254-7257.	1.3	7
103	Initial oxidation behavior of a single crystal superalloy during stress at 1150 °C. Scientific Reports, 2020, 10, 3089.	1.6	7
104	Oxygen changes crack modes of Ni-based single crystal superalloy. Materials Research Letters, 2021, 9, 531-539.	4.1	7
105	Shock-induced α" martensitic transformation in Nb single crystals. Materials Science & Engineering A: Structural Materials: Properties, Microstructure and Processing, 2022, 846, 143274.	2.6	7
106	Revealing the elemental-specific growth dynamics of Pt–Cu multipods by scanning transmission electron microscopy and chemical mapping. Journal of Materials Chemistry A, 2015, 3, 21284-21289.	5.2	6
107	Facile synthesis of hierarchical β-LiFePO4and its phase transformation to electrochemically active α-LiFePO4for Li-ion batteries. CrystEngComm, 2016, 18, 7707-7714.	1.3	6
108	Strain Gradient Modulated Exciton Evolution and Emission in ZnO Fibers. Scientific Reports, 2017, 7, 40658.	1.6	6

#	Article	IF	CITATIONS
109	The dependence of stress and strain rate on the deformation behavior of aÂNiâ€based single crystal superalloy at 1050°C. International Journal of Mechanical System Dynamics, 2021, 1, 121-131.	1.3	6
110	Direct identification of monolayer rhenium diselenide by an individual diffraction pattern. Nano Research, 2017, 10, 2535-2544.	5.8	5
111	Temperature distribution of wedge-shaped specimen in TEM. Micron, 2018, 110, 46-49.	1.1	5
112	Fast Gas–Solid Reaction Kinetics of Nanoparticles Unveiled by Millisecond Inâ€Situ Electron Diffraction at Ambient Pressure. Angewandte Chemie, 2018, 130, 11514-11518.	1.6	5
113	Growth of â€~W' doped molybdenum disulfide on graphene transferred molybdenum substrate. Scientific Reports, 2018, 8, 7396.	1.6	5
114	Towards quantitative mapping of the charge distribution along a nanowire by in-line electron holography. Ultramicroscopy, 2018, 194, 126-132.	0.8	5
115	Direct Observation of Curved Surface Enhanced Disordering in Ag ₂ S Nanoparticles. Journal of Physical Chemistry C, 2019, 123, 940-944.	1.5	4
116	In situ atomistic mechanisms of detwinning in nanocrystalline AuAg alloy. Science China Materials, 2022, 65, 820-826.	3.5	4
117	Crack Propagation Behavior of a Ni-Based Single-Crystal Superalloy during In Situ SEM Tensile Test at 1000 °C. Crystals, 2020, 10, 1047.	1.0	3
118	Spherical to truncated octahedral shape transformation of palladium nanocrystals driven by e-beam in aqueous solution. Nano Research, 2019, 12, 2623-2627.	5.8	2
119	Reversible transformation between terrace and step sites of Pt nanoparticles on titanium under CO and O2 environments. Chinese Journal of Catalysis, 2022, 43, 2026-2033.	6.9	2
120	B12-P-08In situ observation of dislocation accumulation and small angle grain boundary formation. Microscopy (Oxford, England), 2015, 64, i89.1-i89.	0.7	0
121	B21-O-14Ultra-large elasticity and Liquid-like behavior of Nano-materials. Microscopy (Oxford,) Tj ETQq1 1 0.784	314 rgBT 0.7	/Overlock 10
122	B21-P-09The crystal micro-structure evolution of in-situ annealed phase change material TiSbTe film. Microscopy (Oxford, England), 2015, 64, i101.2-i101.	0.7	0
123	B11-O-10In situ Atomic Scale Mechanical Microscopy. Microscopy (Oxford, England), 2015, 64, i15.1-i15.	0.7	0
124	B21-O-05Atomic motion in monolayer molybridenum disulfide probed by in-situ ADF-STEM. Microscopy (Oxford, England), 2015, 64, i41.2-i41.	0.7	0
125	B22-O-12In Situ Atomic Scale Observation of Grain Rotation Mediated by Grain Boundary Dislocations. Microscopy (Oxford, England), 2015, 64, i52.2-i52.	0.7	0
126	B22-P-17Evolution of the MC carbide in Nickel-base single crystal superalloy exposing at 950 °C. Microscopy (Oxford, England), 2015, 64, i111.1-i111.	0.7	0

#	Article	IF	CITATIONS
127	Microscopy sparks development. Nature Materials, 2016, 15, 695-697.	13.3	0
128	Tuning the Outward to Inward Swelling in Lithiated Silicon Nanotubes via Surface Oxide Coating. Microscopy and Microanalysis, 2017, 23, 2018-2019.	0.2	0